

TARA: Thermal-Aware Routing Algorithm for Implanted Sensor Networks^{*}

Qinghui Tang, Naveen Tummala, Sandeep K. S. Gupta¹, and Loren Schwiebert²

¹ Arizona State University, Tempe AZ 85287, USA,
{qinghui.tang, naveen.tummala, sandeep.gupta}@asu.edu

² Wayne State University, Detroit, MI 48202,
loren@cs.wayne.edu

Abstract. Implanted biological sensors are a special class of wireless sensor networks that are used in-vivo for various medical applications. One of the major challenges of continuous in-vivo sensing is the heat generated by the implanted sensors due to communication radiation and circuitry power consumption. This paper addresses the issues of routing in implanted sensor networks. We propose a thermal-aware routing protocol that routes the data away from high temperature areas (hot spots). With this protocol each node estimates temperature change of its neighbors and routes packets around the hot spot area by a withdraw strategy. The proposed protocol can achieve a better balance of temperature rise and only experience a modest increased delay compared with shortest hop, but thermal-awareness also indicates the capability of load balance, which leads to less packet loss in high load situations.

1 Introduction

An implanted biomedical sensor is a device that detects, records and transmits information regarding a physiological change in the biological environment. It also finds its usages in various medical applications like retinal prosthesis [1], and cancer detection. Sensors work cooperatively by exchanging information and monitoring environmental changes, so wireless communication is necessary for reliable data communication amongst sensors.

The routing problem in wireless sensor networks has been well studied. Most of the routing protocols in wireless sensor networks are designed to satisfy power efficiency or delay constraints. None of them consider the possibility of hazardous effects resulting from communication radiation and power dissipation of implanted sensors. In our previous work [2], we show the communication scheduling among sensors should consider the cluster leadership history and sensor locations to minimize thermal effect on the surrounding tissues.

Radio signals used in wireless communication produce electrical and magnetic fields. The human tissue will absorb radiation and experience temperature rise

^{*} This work is supported in part by NSF grants ANI-0086020.

when exposed to electromagnetic fields. Even with modest heating, some organs which are very sensitive to temperature rise due to lack of blood flow to them, are prone to thermal damage (e.g., lens cataract [3]). Continuous operation of sensor circuitry also contributes to the temperature rise of tissues. Specific Absorption Rate (SAR, unit is W/kg) is a measure of the rate at which radiation energy is absorbed by the tissue per unit weight. The relationship between radiation and SAR is given by

$$SAR = \frac{\sigma |E|^2}{\rho} \text{ (W/kg) ,} \quad (1)$$

where E is the induced electric field by radiation, ρ is the density of tissue and σ is the electrical conductivity of tissue. Many countries and organizations set strict standards for peak values of SAR. Experiments show exposure to an SAR of 8W/kg in any gram of tissue in the head or torso for 15 minutes may have a significant risk of tissue damage [4].

In this work, our purpose is to reduce the possibility of overheating and we are the first to consider thermal influence in a sensitive application environment. We demonstrate the thermal effects caused by sensors implanted in a biological body. We first obtain a radiation model of a communication antenna. With the Finite-Difference Time-Domain method (FDTD) we can calculate the temperature rise and SAR of each implanted sensor node by using Pennes bioheat equation [5]. Then we propose Thermal-Aware Routing Algorithm (TARA) to handle packet transmission in the presence of temperature hot spots. Extensive simulations were conducted to verify and compare its performance with shortest hop algorithm. The smaller maximum temperature rise and smaller average temperature rise of TARA indicate that TARA is a safer routing solution for implanted applications. Although our protocol has higher transmission delay, it also introduces less traffic congestion into the network because thermal-awareness of TARA technically equals to load balancing capability (the more traffic a node handles, the more energy is consumed and the more heat is generated. Balancing temperature rise equals to balancing traffic load).

In Section 2, we give a brief overview of related work and classification of the hot spot routing problem. We describe our system model and proposed thermal-aware routing protocol in Section 3. We also discuss how to calculate SAR and temperature rise in Section 3. Simulation results and comparison with shortest hop algorithm is presented in Section 4. We conclude in Section 5.

2 Related Work

Ad-hoc routing has been studied extensively for ad-hoc networks and sensor networks. In most situations, energy-efficiency, delay constraints, and transmission hops are design constraints. Those algorithms are not appropriated for in vivo biomedical sensors since they did not consider that even though some routes are eligible choices for light traffic and shorter delay, the temperature is already so high that further operation of those forwarding nodes is unbearable.

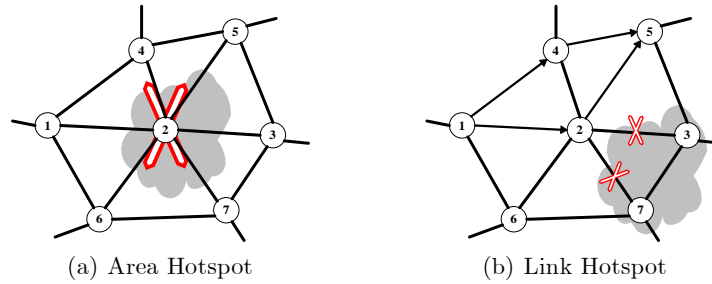


Fig. 1. Difference between area hot spot and link hot spot (a) all links are broken, node 2 is not accessible (b) some links are broken, node 2 is accessible

Thus we realized there are existing two hot spot routing problems in the networking field, namely, **area hot spot** and **link hot spot**. We believe current research on ad-hoc routing or sensor network routing focus only on link hot spot problem where only some network links of a node suffer congestion and packet loss, whereas other links are still available. Figure 1 shows the difference between area hot spot and link hot spot. In the former, the area surrounding node 2 is the hot spot region, and all links connecting with node 2 are disconnected thus node 2 is isolated from network. Whereas in link hot spot as shown in Figure 1(b), only some links connecting node 2 with the outside network are disconnected; node 2 is accessible and qualified as a forwarding node (e.g., route 6->2->5 is still available).

It may seem that since a load balancing routing algorithms distributes packets evenly, implying even distribution of power consumption due to communication and data processing, it can also minimize temperature rise. However, this is not always true. For instance, as shown in Figure 1(b), route $1 \rightarrow 4 \rightarrow 5$ and $1 \rightarrow 2 \rightarrow 5$ can be used to balance traffic. If we assume node 2 already suffers from temperature rise due to previous packet forwarding from node 4 to node 7, then node 2 is no longer available for load balancing and forwarding packets between node 1 and node 5.

Some heuristic protocol, e.g., the clustering-based protocol LEACH [6] can evenly distribute the energy consumption among the sensors in the network on a long term basis (large time scale). But on short term (small time scale), since the rotation of cluster head is made randomly, it is highly possible that some high temperature nodes are selected as the cluster lead. Similarly, the "Energy Equivalence Routing" proposed by Ding *et al.* [7] adjusts routing path periodically to balance energy consumption among sensors, but may not satisfy short time temperature rise criteria. Woo *et al.* [8] suggested link connectivity status (based on wireless signal quality) should be maintained in a neighborhood table regardless of cell density. In our study, link connectivity also depends on environment temperature and node distribution density plays a critical role in temperature change. Estrin *et al.* [9] mentioned that the deployment of sensors

becomes a form of environmental contamination, and the emission of active sensors could be harmful or disruptive to organisms. Thus environmental impact of sensor networks needs to be examined in more details. Our protocol considers such new constraint of implanted applications, and tries to reach load balancing and temperature rise balance in a smaller time scale to reduce bio-safety risk. We expect our work will motivate further research attention in this field. Also we believe there are some similar scenarios where communication or operation of network will cause environmental disturbance which is undesired:

- In **drug development** or **food processing**, some enzymes are used as catalysts or ingredients. Enzymes are extremely sensitive to the change of environment, such as pH value and temperature. Embedded sensors are used for reagent delivery, and quality monitoring or quality control.
- In **protein crystal growth**, Micro-Electro Mechanical Systems (MEMS) and sensors are embedded to control and monitor the growth process [10]. Temperature is one of the critical factors leading to successful crystal growth. Obviously we hope to minimize the heating influence resulting from the operation of embedded MEMS and sensors.

3 Thermal Aware Routing Protocol

3.1 System Model

The temperature surrounding the sensor nodes can be measured by using a temperature sensor inside the sensor node's circuitry, but this will enlarge the sensor size and increase complexity of the sensor circuit. So in our model we assume that we cannot measure the temperature surrounding the sensor node. Temperature is estimated by observing sensor activities. In our model, we assume that the dielectric and perfusion properties of the tissues are known. The locations of the biosensors are predefined as they are physically implanted rather than randomly dropped as in some other sensor applications.

As shown in Figure 2, distributed sensors are implanted inside biological tissues, and continuously generate packets that need to be sent to the edge of the network, where a **gateway node** aggregates data and transmits to a **base station**, which is located outside the body. Each sensor has an omnidirectional antenna and no sensor node is disconnected from the network. We assume no collision happens due to simultaneously transmission.

3.2 Temperature Estimation

We identify two major sources that cause the heating effects: the radiation from the sensor node antenna and the power dissipation of sensor node circuitry.

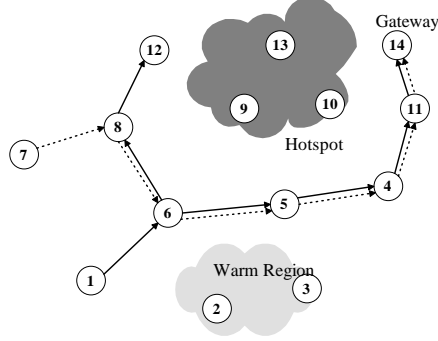


Fig. 2. System model: all data packets are forwarded to the gateway. Nodes inside the hotspot region are disconnected from other nodes

Radiation from the Antenna We assume that the sensor node has a short dipole antenna consisting of a short conducting wire of length dl with a sinusoidal drive current I . To analyze the effect of radiation on the tissue, we assume the tissue to be homogeneous with no sharp edges or rough surfaces. The space around the antenna is divided into near field and far field. The extent of the near field is given by $d_0 = \frac{\lambda}{2\pi}$, and λ is the wavelength of the RF used by wireless communication. SAR in the near field and far field is given by [11]:

$$SAR_{NF} = \frac{\sigma\mu\omega}{\rho\sqrt{\sigma^2 + \epsilon^2\omega^2}} \left(\frac{Idl \sin\theta e^{-\alpha R}}{4\pi} \left(\frac{1}{R^2} + \frac{|\gamma|}{R} \right) \right)^2 \quad (2)$$

and [12]:

$$SAR_{FF} = \frac{\sigma}{\rho} \left(\frac{\alpha^2 + \beta^2}{\sqrt{\sigma^2 + \omega^2\epsilon^2}} \frac{Idl}{4\pi} \right)^2 \frac{\sin^2\theta e^{-2\alpha R}}{R^2} . \quad (3)$$

where R is the distance from the source to the observation point, θ is the angle between the observation point and the x-y plane, and γ is the propagation constant³.

We assume our two-dimensional control volume located at the x-y plane and the control volume is perpendicular to the small dipole, thus we can safely assume the radiation pattern is omnidirectional on the 2D plane and $\sin\theta = 1$. The near field or the far field radiation of the sensor's transmitter causes the heating of the tissue because of the absorption of the radiation. The Specific Absorption Rate is used to estimate the potential heat effect on the human tissue.

Power dissipation by Sensor node circuitry The power dissipation of sensor circuitry will raise the temperature of sensor nodes. The power consumed

³ given by $\gamma = \alpha + j\beta$, phase constant β is given as [13] $\beta = \omega\sqrt{\frac{\mu\epsilon}{2}} \left[\sqrt{1 + \left(\frac{\sigma}{\omega\epsilon}\right)^2} + 1 \right]^{1/2}$ (rad/m).

by the sensor circuitry divided by the volume of sensor, is the power dissipation density, denoted as P_c , which depends on its implementation technology and architecture. In our analysis, we have considered the typical power consumption for a regular sensor circuitry operation.

3.3 Calculating Temperature Rise

The above mentioned sources of heating the tissue can cause a rise of temperature of the sensor and its surrounding area. The rate of rise in temperature is calculated by using the Pennes bioheat equation [5] as follows:

$$\rho C_p \frac{dT}{dt} = K \nabla^2 T + \rho SAR - b(T - T_b) + P_c + Q_m \text{ (W/m}^2\text{)}. \quad (4)$$

In this equation, ρ is the mass density, C_p is the specific heat of the tissue, K is the thermal conductivity of the tissue, b is the blood perfusion constant, which indicates how fast the heat can be carried away by blood flow inside the tissue, and T_b is the temperature of the blood and the tissue.

On the left side of Eq. (4), $\frac{dT}{dt}$ is the rate of temperature rise in the control volume. Terms on the right side indicate the heat accumulated inside the tissue. $K \nabla^2 T$ and $b(T - T_b)$ are the heat transfer due to the conduction and the blood perfusion, respectively. ρSAR , P_c and Q_m are the heat generated due to the radiation, the power dissipation of circuitry, and the metabolic heating, respectively

Finite-Difference Time-Domain (FDTD) [14] is an electromagnetic modeling technique that discretizes the differential form of time and space, which can also be used for heating application. The entire problem space is discretized into small grids. Each grid is marked with a pair of coordinates (i, j) . Due to space limitation, we show only the result of the new bioheat equation after some manipulations:

$$\begin{aligned} T^{m+1}(i, j) = & \left[1 - \frac{\delta_t b}{\rho C_p} - \frac{4\delta_t K}{\rho C_p \delta^2} \right] T^m(i, j) \\ & + \frac{\delta_t}{C_p} SAR + \frac{\delta_t b}{\rho C_p} T_b + \frac{\delta}{\rho C_p} P_c \\ & + \frac{\delta_t K}{\rho C_p \delta^2} \left[T^m(i+1, j) + T^m(i, j+1) \right] \\ & \quad \left[+ T^m(i-1, j) + T^m(i, j-1) \right], \end{aligned} \quad (5)$$

where $T^{m+1}(i, j)$ is the temperature of the grid (i, j) at time $m+1$, and δ_t is discretized time step, δ is the discretized space step (i.e., the size of the grid).

From (5), we can find the temperature of the grid point (i, j) at time $m+1$, which is a function of the temperature at grid point (i, j) at time m , as well as a function of the temperature of surrounding grid points $((i+1, j), (i, j+1), (i-1, j), \text{ and } (i, j-1))$ at time m . Once we know the properties of the tissue, the properties of blood flow, and the power or heat absorbed by the tissue, we can estimate the temperature at a given time and whether the heat effects would cause any damage to the surrounding tissues.

3.4 Protocol Description

In our protocol the forwarding is based on localized information of the temperature and hop counts to the destination. High temperature node identified as hot spot by its neighbors, and this information will be spread to other nodes by withdrawn packets. Once the temperature drops down, the neighboring node will inform other nodes about the new availability of the path.

Setup Phase In the setup phase, by exchange neighborhood information, each sensor collects information to form its own neighbor nodes list, and also knows the number of hops to other nodes and who is the next hop for a specified destination address.

Data Forwarding Each node sends a reading to the gateway node in either of these two circumstances: when there is a change in the sensed reading or when a base station sends a signal to the node asking for the data. It is assumed that each node knows the location of the gateway. When a node receives a packet that is destined to the gateway, it selects the next node based on the minimal temperature criteria. Any packets destined to the hot spot node will be buffered until the estimated temperature drops. If the buffered packet exceeds its time constraint, it is dropped. Any packet whose destination is not a hot spot node but the next hop is hot spot will be withdrawn and returned to the previous hop node.

Hot spot Detection Each node listens to its neighbors' activity, counting the packets they transmitted and received. Based on this activity each node can evaluate the communication radiation and power dissipation of its neighbors, and estimate their temperature changes by using FDTD. Once the temperature of one neighbor exceeds a predefined threshold, the node would mark that neighbor as a hot spot. Also, if no activity happens the temperature of the neighbor will gradually drop, and the neighbor will be removed from the hot spot list once its temperature is beneath some threshold.

To reduce network overhead and save energy the node will not actively broadcast the hot spot information to other nodes. But if the temperature drops beneath the threshold, the node will notify its neighbor of this new availability information.

Withdrawal In certain circumstances, a node might receive a packet where it does not have any next hop to forward to or all the nodes in the forwarding set are in the hot spot region. During such a situation, the node returns the packet to the previous node. The previous node tries to forward the packet to another available next hop node, or returns the packet to its previous node if no next hop available. Hot spot information will be carried with packets to inform precedent nodes about the hot spot. If a node (namely, **A**) send a withdraw packet to another node (namely, **B**), when temperature drops down later, node A is responsible for notifying B that the clear of the hot spot.

Table 1. Parameters and their values used in Simulation

Parameter	Property	value
ϵ_r	Relative permittivity at 2MHz or 2.45GHz	826 or 52.73
P_{NL}	Power consumption of non-leader sensor node	1mW
C_p	Specific heat	3600 $\frac{J}{kg^\circ C}$
K	Thermal conductivity	0.498 $\frac{J}{m.s^\circ C}$
b	Blood perfusion constant	2700 $\frac{J}{m^3.s^\circ C}$
T_b	Fixed blood temperature	37 $^\circ C$
ρ	Mass density	1040 $\frac{kg}{m^3}$
σ	Conductivity at 2MHz or 2.45GHz	0.5476 or 1.7388 $\frac{S}{m}$
P_L	Power consumption of Leader node	5 mW
T_1	Leader Time	600 sec
δ	Control Volume cell size	0.005 m
δ_t	Time step of FDTD	10 sec
I_0	Current provided to sensor node antenna	0.1 A

Example As shown in Figure 2, when node 1 has a packet for node 14, it chooses node 6 since node 2 is inside the warm region, which means that the temperature is above the normal temperature but not as critical as hot spots. When the packet reaches node 12 through the path 1→6→8→12, computation of temperature at node 12 reveals that the temperature of the next hop is too high to perform any forwarding operation. Then node 12 returns the packet along its origin route, until a node has a next hop available to forward data (node 6 in this case). During this withdrawal phase the packet direction is set to be negative. Any node receiving a negative direction packet knows that it is a back routed packet and updates within itself the hot spot information obtained from the packet (the high temperature at node 9 and node 13). Now if the node 7 has a packet for node 14, it sends the packet to node 8, which should forward the packet to node 12. But the hot spot information obtained from the previous withdrawal packet makes node 8 select node 6 as a next hop.

4 Simulation

We modeled a two-dimensional area with 12 nodes implanted. The simulation program was developed on Matlab. We use the tissue properties and wave propagation characteristics shown in Table 1. We used various scenarios with different node locations and took the average to plot the graphs. We compared shortest hop protocol with our approach as it demonstrates the trade-off. Maximum temperature rise and average temperature rise are used as metrics for measuring the performance of the proposed protocol.

Maximum Temperature Rise is the highest temperature rise inside the whole network area. It captures the effectiveness of a routing protocol to direct data away from the hot spots. As shown in Figure 3, the maximum temperature

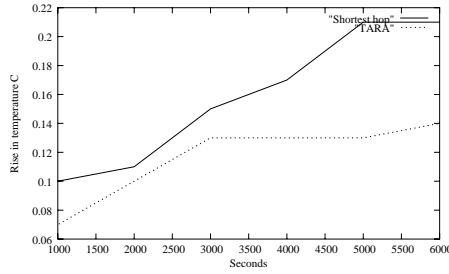


Fig. 3. Maximum temperature rise of TARA (*dotted line*) is lower than that of Shortest hop (*solid line*) because TARA directs packets away from hotspot area

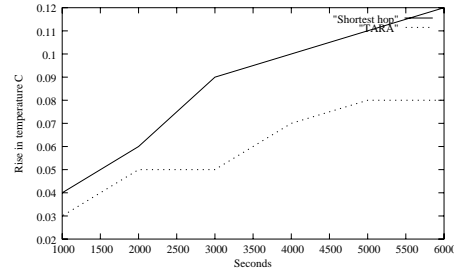


Fig. 4. Average temperature rise of TARA (*dotted line*) is lower than that of Shortest path (*solid line*) because the latter excessively uses the same path

rise of TARA is much lower than the shortest hop, which can be attributed to TARA's selecting the next node that has the least temperature residue and avoiding further deterioration of the overheated area.

Average Temperature Rise is used to estimate the average amount of heat generated at each point inside the network. As shown in Figure 4, TARA has a lower average temperature than the shortest hop whose continuing usage of the same shortest path creates an overheated area.

Notice that in Figure 3, TARA experiences a flat temperature history during time period from 3000 seconds to 5000 seconds. This can be explained as: because part of the network reaches the temperature threshold, TARA is trying to route packets through other low temperature area, thus the peak temperature of network is keeps unchanged; at the same time period, average temperature is still rising as shown in Figure 4 since network operation is continuously introducing heat into the network.

Figure 5 and Figure 6 demonstrate the temperature rise distribution inside the network. Figure 5 demonstrates that temperature rise is relatively evenly distributed in the whole area since the thermal-awareness of TARA avoids introducing the overheated area. Several temperature peaks of Figure 6 indicate the unawareness of the overheated area of the Shortest Hop algorithm, which may lead to thermal damage to human tissues. We also notice that the gateway node at coordinates (6, 6) is always experiencing the highest temperature rise since it is responsible for gathering and forwarding all data to basestation. In practice, the gateway node is located near the surface of the body, where better heat conduction and ventilation will counteract the overheating problem.

Delay Performance In this section, we explain the simulation results of our protocol implemented on **Crossbow MICA2** sensor motes. The aim is to demonstrate the trade-off between delay/throughput and temperature rise. We use the average delay and percentage of packets meeting the deadline as the metrics to demonstrate the performance of protocols. First, we introduce only

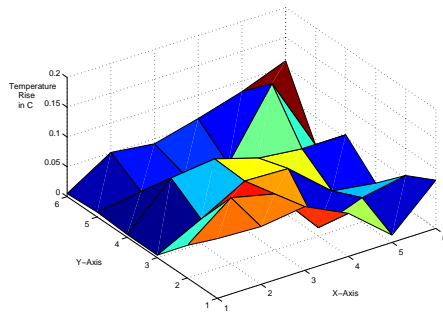


Fig. 5. Temperature distribution of TARA: temperature rise is relatively even in the whole area since the thermal-awareness of TARA avoids introducing the overheated area

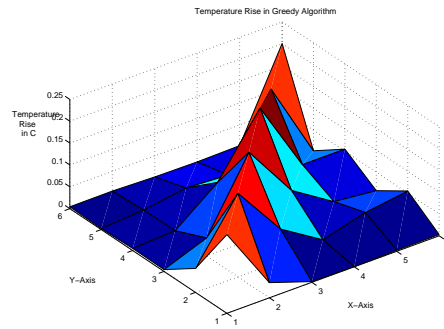


Fig. 6. Temperature distribution of Shortest Hop: several temperature peaks indicate the unawareness of the overheated area

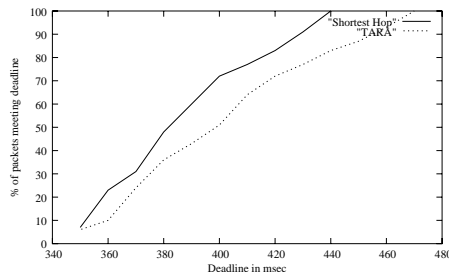


Fig. 7. Performance of TARA and Shortest Hop with only one constant traffic flow traveling across the network, TARA experiences a higher loss due to larger delay

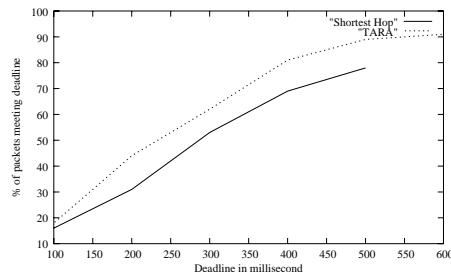


Fig. 8. Delay performance with low traffic: unlike Shortest Hop, thermal-awareness of TARA equals to load balancing, thus fewer packets are lost due to congestion

one constant flow of traffic, travelling across the network. As shown in Figure 7, for various deadline constraints, more packets of Shortest Hop meet the deadline than that of TARA because its packets travel along the shortest path, and TARA experiences a higher loss due to larger delay.

Secondly, we introduce randomly generated traffic of about 100 bytes/second from different nodes of the network. From Figure 8 we can see more packets of TARA meet the delay deadline than that of Shortest Hop. This is because the greedy approach of Shortest Hop results in congestion in some shortest paths, whereas TARA's thermal-awareness also indicates its load balancing capability which results in less congestion and less packet loss.

When the deadline is shorter than 400 millisecond, under the same percentage of packets meeting deadline, e.g., 70%, our proposed protocol only experiences

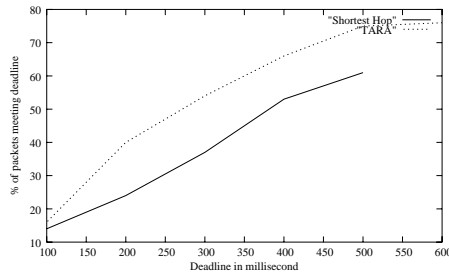


Fig. 9. Delay performance with high traffic: unlike Shortest Hop, thermal-awareness of TARA equals to load balancing, thus fewer packets are lost due to congestion

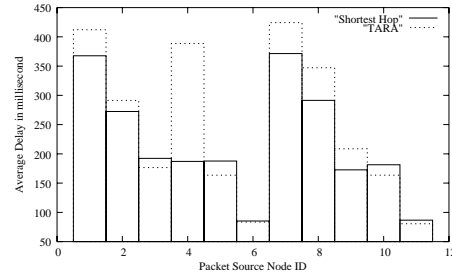


Fig. 10. Although Shortest Hop experiences higher packet loss, but those survived packets have smaller transmission delay compared with TARA

a modest increase in packet delivery times (50 millisecond) while evenly distributing load among the sensors to satisfy the temperature rise constraint.

Figure 9 shows the percentage of packets meeting the deadlines with a higher traffic of about 250 bytes/second. TARA still has a higher percentage of packets meeting the deadline than shortest-hop routing. Figure 8 and Figure 9 also conclude that TARA can achieve load balancing and temperature rise balance simultaneously.

Although the shortest hop algorithm has higher packet losses, from another perspective, those packets who survive the congestion and the buffer overflow have smaller delay. To demonstrate this, we also calculated the average delay for packets generated from different nodes. As shown in Figure 10, average packet delay of Shortest Hop is smaller than TARA. But it also shows that TARA from different source nodes only suffers a modest delay than that of Shortest Hop routing. This means TARA is promising at reaching temperature rise balancing without significant degradation on delay performance.

5 Conclusion

This paper presents a new thermal-aware routing protocol TARA for implanted biosensor networks. TARA takes into consideration the heating factors resulting from the operation of sensor nodes and routes data to minimize thermal effects in a heat-sensitive environment. It also introduces less traffic congestion in the network because thermal-awareness of TARA technically equals to a load balancing capability. TARA is compared with a shortest-hop routing protocol. The smaller maximum temperature rise and average temperature rise of TARA indicate that TARA is a safer routing solution for implanted applications without significant degradation on delay performance. Next, we will improve the TARA protocol to consider more design constraints, such as multipath routing [15], energy consumption, link distance among sensors and the channel estimation

mechanism. We will extend our investigation by comparing TARA with other routing protocols in terms of energy-efficiency, overhead, recovery time, etc.

References

1. Schwiebert, L., Gupta, S.K.S., Auner, P.S.G., Abrams, G., Lezzi, R., McAllister, P.: A biomedical smart sensor for visually impaired. In: *IEEE Sensors 2002*, Orlando, FL., USA (2002)
2. Tang, Q., Tummala, N., Gupta, S.K.S., Schwiebert, L.: Communication scheduling to minimize thermal effects of implanted biosensor networks in homogeneous tissue. *IEEE Tran. Biomedical Eng.* (accepted for publication)
3. Hirata, A., Ushio, G., Shiozawa, T.: Calculation of temperature rises in the human eye for exposure to EM waves in the ISM frequency bands. In: *IEICE Trans. Comm. Volume E83-B.* (2000) 541–548
4. International Electrotechnical Commission IEC: *Medical Electrical Equipment, Part 2-33: Particular Requirement for the Safety of Magnetic Resonance Systems for Medical Diagnosis IEC 60601-2-33.* 2nd edn. (1995)
5. Pennes, H.H.: Analysis of tissue and arterial blood temperature in the resting human forearm. *Journal of Applied Physiology* **1.1** (1948) 93–122
6. Heinzelman, W.R., Chandrakasan, A., Balakrishnan, H.: Energy-efficient communication protocol for wireless microsensor networks. In: *Proc. 33rd Hawaii Int'l Conf. System Sciences. Volume 8.*, IEEE Computer Society (2000) 8020
7. Ding, W., Iyengar, S.S., R. Kannan and, W.R.: Energy equivalence routing in wireless sensor networks. *Journal of Microcomputers and Applications: Special issue on Wireless Sensor Networks* (2004)
8. Woo, A., Tong, T., Culler, D.: Taming the underlying challenges of reliable multipath routing in sensor networks. In: *SenSys '03*, ACM Press (2003) 14–27
9. Estrin, D., Michener, W., Bonito, G.: Environmental cyberinfrastructure needs for distributed sensor networks. A report from a national science foundation sponsored workshop (2003)
10. Tseng, F.G., Ho, C.E., Chen, M.H., Hung, K.Y., Su, C.J., Chen, Y.F., Huang, H.M., Chieng, C.C.: A chip-based-instant protein micro array formation and detection system. In: *Proc. NSTI Naotech'04. Volume 1.*, Boston (2004) 39–42
11. Prakash, Y., Lalwani, S., Gupta, S.K.S., Elsharawy, E., Schwiebert, L.: Towards a propagation model for wireless biomedical applications. In: *IEEE ICC 2003. Volume 3.* (2003) 1993–1997
12. National Council on Radiation and Measurements: *A Practical Guide to the Determination of Human Exposure to Radio Frequency Fields.* Report no. 119. NCRP, Bethesda, MD (1993)
13. Ulaby, F.T.: *Fundamentals of Applied Electromagnetics.* Prentice-Hall (1999)
14. Sullivan, D.M.: *Electromagnetic Simulation Using the FDTD Method.* IEEE Press (2000)
15. Ganesan, D., Govindan, R., Shenker, S., Estrin, D.: Highly-resilient, energy-efficient multipath routing in wireless sensor networks. *SIGMOBILE Mob. Comput. Commun. Rev.* **5** (2001) 11–25